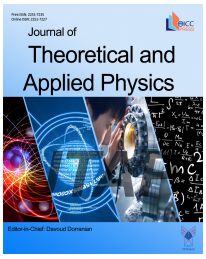

Volume 17, Issue 5, 172347 (1-9)

Journal of Theoretical and Applied Physics (JTAP)

https://dx.doi.org/10.57647/j.jtap.2023.1705.47

Elastic moduli of some rare-earth doped tellurite glasses

Raouf El-Mallawany[1]*, Samir A. Yousef[1], Abdelhamid.El-Shaer[2], Hanan A. Elabd[1]

[1]*Physics Department, Faculty of Science, Menoufia University, Menoufia, Egypt.*
[2]*Physics Department, Faculty of Science, Kafreelshikh University, Kafreelshikh, Egypt.*

***Corresponding author**: raoufelmallawany@yahoo.com

Received 06 May 2023; Accepted 31 July 2023; Published Online 04 August 2023 ORIGINAL RESEARCH

Abstract:
Samarium oxide (Sm_2O_3) and ytterbium oxide (Yb_2O_3) doped tungsten-tellurite glasses (TWSm), (TWYb) in the forms of 80 (TeO_2)-(20 − x)(WO_3)−x(Sm_2O_3) and 80 (TeO_2)-(20 − x)(WO_3)−x(Yb_2O_3) with x = 0, 1.0, 2.0, 3.0, 4.0 and 5.0 mol% were prepared by the melt-quenching technique. The XRD analysis for the two prepared glass systems verified the samples' amorphous nature. The glass density (ρ) was measured by the Archimedes method. Both (ρ) and the molar volume (V_M) of the two prepared systems showed an increase with increasing the concentrations of dopants Sm^{3+} and Yb^{3+}. Longitudinal V_L and shear V_S wave velocities were measured at 5 MHz frequency using the pulse-echo technique. Longitudinal (L), shear (G), bulk (K), and Young's moduli (E) have been founded. Moreover, Poisson's (σ), Debye temperature (θ_D), softening temperature (T_S), micro-hardness (H) have been founded for every glass sample. Elastic moduli showed an increase with increasing dopants concentration of (Sm_2O_3) or (Yb_2O_3). Moreover, the bulk modulus of (TWSm) glasses was higher than (TWYb) glasses. Mechanical properties of (TWSm) and (TWYb) are crucial parameter in manufacturing optical fibers.

Keywords: Glasses; Tellurite; Rare earth; Elastic moduli

1. Introduction

Tellurite glasses have been considered smart materials due to their unique physical properties and will be a candidate for sophisticated applications in comparison with other glasses [1–14]. Doping with rare earth (R.E.) or transition metal (T.M.) oxides induced changes in the glass structure and produced new physical properties for laser-fiber amplifier applications, color-changing in germano-tellurite niobate glass, 2–3 μm mid-infrared luminescence, and Nd^{3+}-doped for transparent tellurite ceramics bulk lasers [15–19]. While in the year 2022, many researchers have been attracted to tellurite glasses in different ways like; spectroscopic measurements for solid-state lighting applications, fabrication, laser materials, magneto-optic fiber current sensors, and LED applications.
Knowledge of the mechanical properties of glass is necessary for the majority of glass's technological applications. Synthesize (TWSm), (TWYb) glasses and measuring the elastic moduli of some (RE) doped tungsten-tellurite glasses are the motivation and novelty of the present work because elastic moduli (L), (G), (K), (E) are crucial parameter in manufacturing optical fibers. Moreover, (σ), (θ_D), (T_S), (H), (d), and (Z) will be calculated.

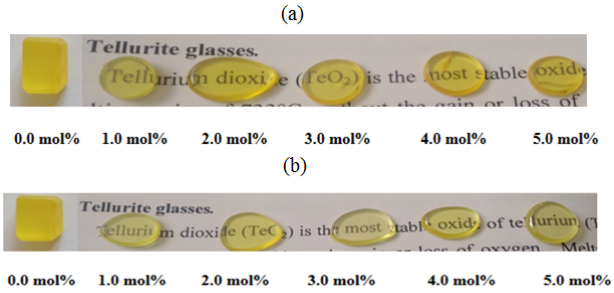

Figure 1. Photographs of the prepared samples: (a) for TWSm glass system and (b) for TWYb glass system.

2. Experimental work

Two tellurite glass series have been synthesized (TWSm) and (TWYb). Oxides of high purity of tellurium dioxide, TeO_2 (Alfa Aesar 99.99), WO_3 (Alpha Chemika 99.9), Sm_2O_3 (SIGMA-Aldrich 99.9), and Yb_2O_3 (SIGMA-Aldrich 99.9) in specified weights were taken and grounded

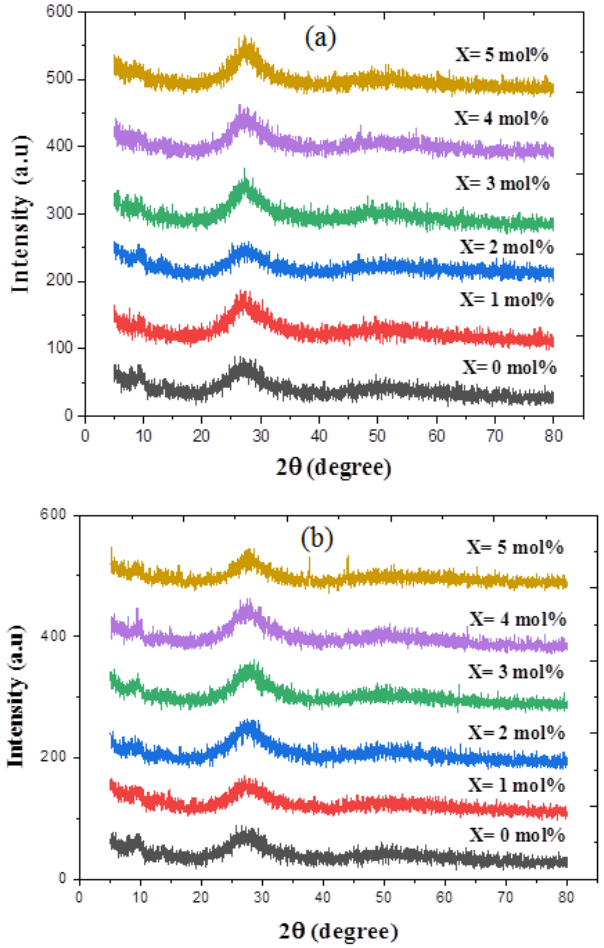

Figure 2. (a) XRD pattern of TWSm glass system and (b) of TWYb glass system.

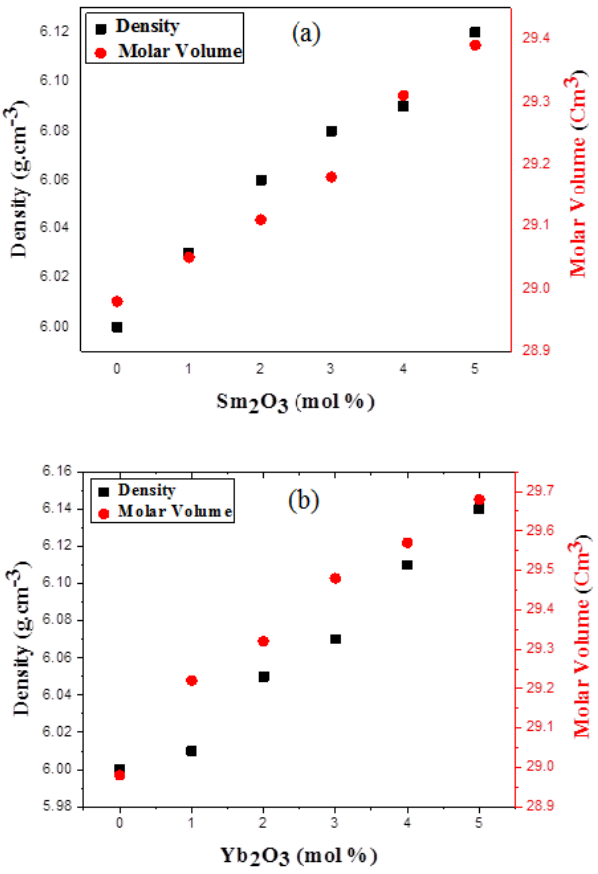

Figure 3. (a) Density and molar volume of TWSm glasses and (b) of TWYb glasses.

using agate mortar for 15 minutes to get a homogeneous mixture. The batches were collected in a ceramic crucible which was preheated in the furnace up to 400ºC for 30 min to reduce the tendency of vitalization. Stirring was done every 10 minutes to remove bubbles and ensure the homogeneity of the melt. The temperature was raised to 850ºC depending on the glass composition. The glasses were cast rapidly into a pre-heated stainless mold (350ºC) to remove thermal strains and then transferred to the annealing furnace at 290ºC (1 hour). The annealed glass samples were polished for physical measurements. XRD Shimadzu diffractometer with Cu Kα radiation at 0.154 nm has been used to confirm the amorphous state.

The glass density has been calculated at room temperature by the next equation:

$$\rho = \left(\frac{W_a}{W_a - W_t}\right)\rho_t \qquad (\mathrm{g.cm^{-3}}) \tag{1}$$

where ρ_t refers to the density of toluene, ρ = glassdensity, W_a is taken as the weight of the glass in air and W_t in toluene. Molar volumes (V_M) have been calculated according to:

$$V_M = \frac{M}{\rho} \qquad (\mathrm{cm^{-3}/mol}) \tag{2}$$

The ultrasonic velocities were measured by using the pulse-echo technique where the time intervals of two echoes were recorded by using Krautkramer USM 36 L model. The velocity was consequently obtained:

$$v = \frac{2d}{\Delta t} \qquad (\mathrm{cms^{-1}}) \tag{3}$$

where d = thickness of samples (cm), and Δt is the transit time between two successive echoes.

Elastic moduli (EM);

$$(L) = V_L^2\rho, \qquad (G) = V_S^2\rho,$$

$$(K) = L - \frac{4}{3}G, \qquad (E) = 2G(1+\sigma),$$

$$(\sigma) = \frac{L-2G}{2(L-G)}, \qquad (\theta_D) = 251.2V_m\left(\frac{nM}{\rho}\right)^{\frac{1}{3}},$$

$$(H) = \frac{(1-2\sigma)E}{6(1+\sigma)}, \qquad (T_S) = \frac{V_S^2 M}{\psi^2 n},$$

$$(V_m) = \left[\frac{1}{3}\left(\frac{1}{V_l^3} + \frac{2}{V_S^3}\right)\right]^{-\frac{1}{3}}, \qquad d = \frac{4G}{k},$$

and $Z = \rho V_l$.

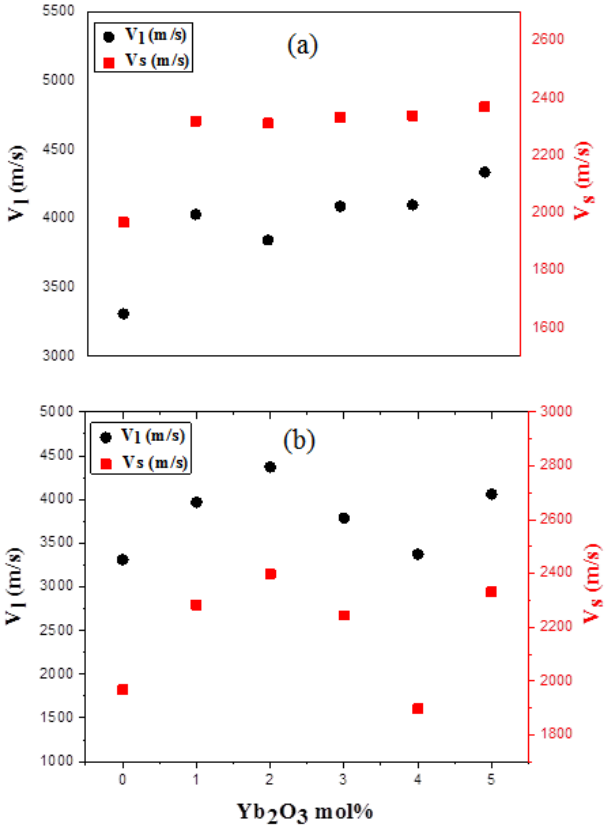

Figure 4. Longitudinal velocity (V_L) and shear velocity (V_S) of (a) TWSm glasses and (b) TWYb glass system.

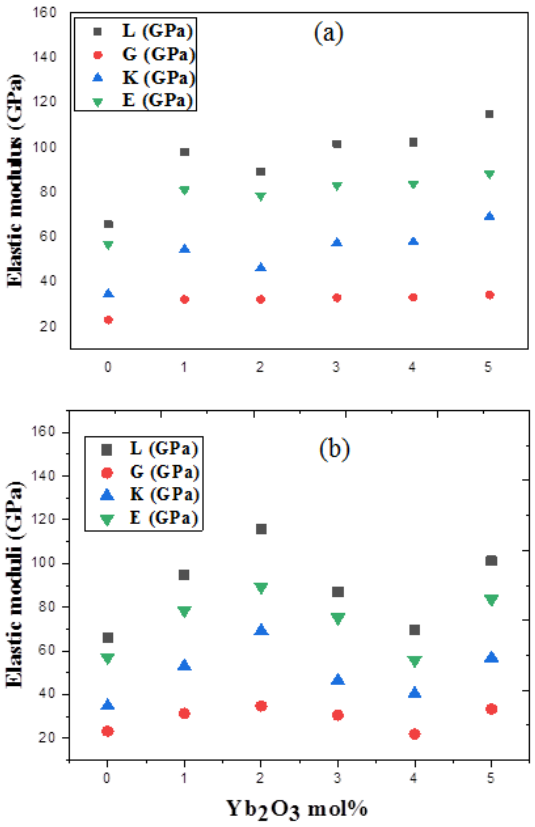

Figure 5. Elastic modulus of (a) TWSm glass system and (b) of TWYb glass system.

3. Results and discussion

The produced glasses were clear, transparent, and have yellowish color for the two glass systems (TWSm) and (TWYb) as shown in Figure 1. While the X-ray diffraction profile of the prepared glasses with no sharp peaks is in Figure 2. Both (ρ) and (V_M) of the (TWSm) and (TWYb) are represented in Figure 3. Values of (ρ) and (V_M) for Sm glass system are found in the range 6.00 g.cm^{-3} to 6.12 g.cm^{-3} and 28.98 (cm^3.mol^{-1}) to 29.39 (cm^3.mol^{-1}) respectively as shown in Table 1. Also, in the case of Yb glass system, these

Table 1. Density and molar volume of (TWSm), (TWYb) glasses.

X Sm_2O_3 (mol%)	(ρ) g.cm^{-3}	(V_M) cm^3.mol^{-1}
0.0	6.0057	28.98
1.0	6.0296	29.05
2.0	6.0601	29.11
3.0	6.0851	29.18
4.0	6.0967	29.31
5.0	6.1201	29.39
X Yb_2O_3 (mol%)		
0.0	6.0057	28.98
1.0	6.011	29.22
2.0	6.0472	29.32
3.0	6.07	29.48
4.0	6.105	29.57
5.0	6.138	29.68

Table 2. Longitudinal, shear and mean ultrasound velocities of (TWSm), (TWYb) glasses.

X Sm_2O_3 (mol%)	V_L (m/s)	V_S (m/s)	V_m (m/s)
0.0	3309	1967	2177
1.0	4031	2319	2575
2.0	3844	2312	2557
3.0	4089	2333	2592
4.0	4100	2338	2598
5.0	4337	2370	2642
X Yb_2O_3 (mol%)			
0.0	3309	1967	2177
1.0	3969	2283	2535
2.0	4371	2398	2673
3.0	3788	2244	2485
4.0	3375	1896	2109
5.0	4061	2332	2590

Table 3. Experimental values of elastic moduli, Poison's ratio (σ), Micro hardness (H), of (TWSm), (TWYb) glasses.

X Sm_2O_3 (mol%)	EM (GPa)				(σ)	(H) (GPa)
	L	**G**	**K**	**E**		
0.0	65.76	23.24	34.78	57.01	0.227	4.23
1.0	97.97	32.43	54.74	81.24	0.253	5.35
2.0	89.54	32.39	46.35	78.82	0.217	6.12
3.0	101.74	33.12	57.58	83.38	0.258	5.33
4.0	102.49	33.33	58.05	83.92	0.259	5.35
5.0	115.12	34.38	69.28	88.49	0.287	4.88
X Yb_2O_3 (mol%)						
0.0	65.76	23.24	34.78	57.01	0.227	4.23
1.0	94.69	31.33	52.92	78.49	0.253	5.16
2.0	115.53	34.77	69.17	89.35	0.285	4.99
3.0	87.01	30.57	46.34	75.17	0.229	5.51
4.0	69.54	21.95	40.28	55.72	0.269	3.37
5.0	101.23	33.38	56.72	83.72	0.254	5.47

values are found in the range 6.00 g.cm^{-3} to 6.13 g.cm^{-3} and 28.98 (cm^3.mol^{-1}) to 29.68 (cm^3.mol^{-1}) respectively as shown in Table 1. For both systems, the values are found to increase as the amount of Sm_2O_3 and Yb_2O_3 is increased. Sm_2O_3 and Yb_2O_3 ions have high molecular weights than other oxide ions in the glass composition (TeO_2 = 159.6 g/mol, WO_3 = 231.84 g/mol, Sm_2O_3 = 348.72 g/mol and Yb_2O_3 = 394.08 g/mol). So, the replacement of WO_3 ions by Sm_2O_3 or Yb_2O_3 ions increases molecular weight and density. Depending on how the samarium ions or ytterbium ions settle themselves in the network, there are various explanations for this increase. The Sm^{3+} and Yb^{3+} ions may fill the network's interstitial spaces, which would result in structural compaction and an increase in density [20–36].

Longitudinal V_L and shear V_S ultrasonic velocities of TWSm glass samples are found in the range of 3309 – 4337 m/s and 1967 – 2370 m/s, respectively. While in the case of the TWYb glass system, the calculated ultrasonic longitudinal and shear velocities values are found in the range of 3309 – 4061 m/s. Table 2 and Figure 4 show the variation of the ultrasonic longitudinal and shear velocities with varying Sm_2O_3 and Yb_2O_3 mol%. As shown in Figure 4(a), for TWSm glass system, at $y = 1$ Mole fractions the two velocities exhibit an expected reduction from 4031 m/s to 3844 m/s and 2319 m/s to 2312 m/s, respectively. In the TWYb glass system shown in Figure 4(b), the two velocities showed an increasing trend with the Yb^{3+} (2 mol%), then decreased at concentrations 3 and 4 mol% and begin to in-

Table 4. Softening temperature (T_S), Debye temperature (θ_D), Fractal bond connectivity (d) and acoustic impedance (Z) of (TWSm), (TWYb) glasses.

X Sm_2O_3 (mol%)	T_S (k)	θ_D (K)	d	$Z \times 10^7$ (Kg m^{-2} s^{-1})
0.0	817	262	2.67	1.99
1.0	1140	310	2.37	2.43
2.0	1137	308	2.76	2.32
3.0	1162	312	2.30	2.49
4.0	1171	313	2.29	2.50
5.0	1207	318	1.98	2.65
X Yb_2O_3 (mol%)				
0.0	817	262	2.67	1.99
1.0	1107	304	2.37	2.39
2.0	1229	321	2.01	2.64
3.0	1083	298	2.64	2.29
4.0	778	253	2.18	2.06
5.0	1183	310	2.35	2.49

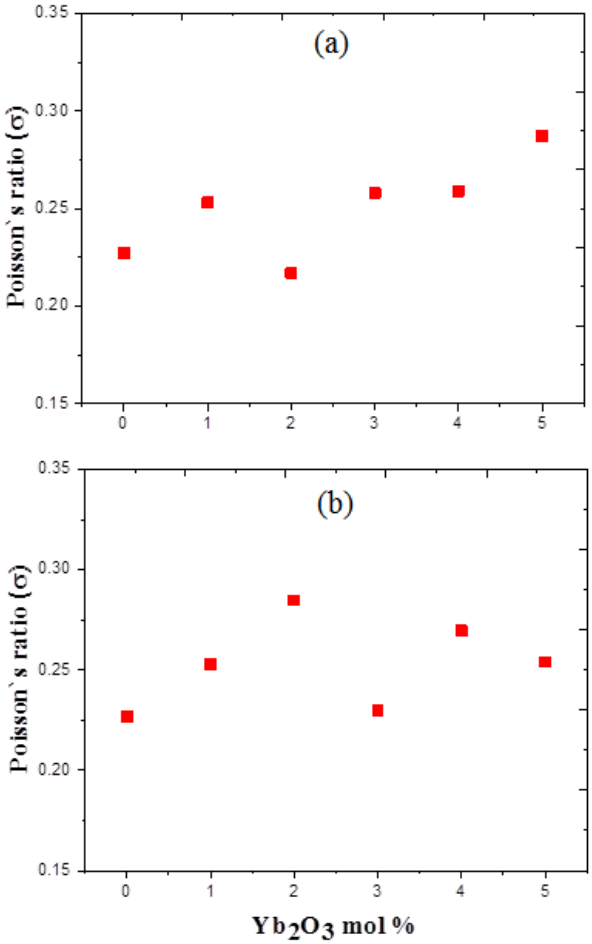

Figure 6. Poisson's ratio of (a) TWSm glasses and (b) of TWYb glasses.

crease again at 5 mol%. Both V_L and V_S could be compared with other glass series [20–35].

Table 3, Table 4, and Figures 5-9 show the variation of (EM) for both (TWSm) and (TWYb) glass series. For (TWSm) glass series; longitudinal modulus (L), 65.76 – 115.12 GPa, Young's modulus (E), 57.01 – 88.49 GPa, bulk modulus (K), 34.78 – 69.28 GPa, and shear modulus (G), 23.24 – 34.38 GPa. in the case of (TWSm) glass system. For (TWYb) glass series, the longitudinal modulus, L, 65.76 – 101.23 GPa, Young's modulus, E, 57.01 – 83.72 GPa, bulk modulus, K, 34.78 – 56.72 GPa and shear modulus, G, 23.24 – 33.38 GPa. With an increase in velocity or density, the (elastic modulus) EM increases. For the TWYb glass, EM showed an increasing trend with the Yb^{3+} mol% until 2.0 mol%, then decreased and increased again at a concentration of 5 mol%. Therefore, for these samples, the network bond type has a vital role in determining the (EM) rather than the density. The present values of bulk modulus are in the range with other tellurite glasses; $60B_2O_3.10Na_2O.20TeO_2.(10-x)$ CaO-$xZrO_2$, $[(TeO_2)0.7(B_2O_3)0.3)0.7(ZnO)0.3]1-x(SrO)x$, SrO-$B_2O_3$-$TeO_2$-$V_2O_5$-$MnO_2$-$MoO_3$-$Tl_2O_3$, B_2O_3-TeO_2-Al_2O_3-ZnO-MgO-Li_2O, xEu_2O_3-5PbO-$25TeO_2$-$(70-x)B_2O_3$, $[(TeO_2)0.7\ (B_2O_3)0.3]1-x\ [MnO_2]x$, xNb_2O_5-$(1-x)TeO_2$, $12Bi_2O_3$-8BaO-12ZnO-$0.5CeO_2$-$17.5SiO_2$-$(50-x)\ B_2O_3$-$xTeO_2$ glasses with x = 0, 10, 20, 30 and 40 mol [27, 28, 30–32, 34–36] and far away from $75TeO_2$-$5Na_2O$-$(20-x)TiO_2$-xBaO and GeO_2-TeO_2-Ga_2O_3 [29, 33].

Values of (σ), (θ_D), (T_S), micro-hardness (H), f (d), and (Z) for both series. For TWSm samples, (σ), increased from 0.227 at $y = 0$ M fraction to 0.287 at $y = 5$ mol%. A slight decrease is observed for (σ), at $y = 2$ M fraction respectively. Similar behavior is observed in TWYb samples but here the decrease in (σ), is observed at concentrations 3 and 5 mol%. Poisson's ratio depends on both the density of the cross-links and the dimension of the glass network. Also, showed (H) increased from 4.23 GPa to 6.12 GPa as Sm^{3+} increases from 0.0 to 2.0 mol% in the TWSm. Microhardness decreases from 5.33 to 4.88 GPa. Figure 7(b) showed the variation of the microhardness (H) in the TWYb glass system. It's observed that (H) has an increasing trend from 4.23 to 5.51 GPa. Meanwhile, the decrease is observed at $y = 2$ and 4 mol%, respectively. Besides that, (T_S), (θ_D), (d), and (Z) for both (TWSm) and (TWYb) glass series. In TWSm glass system, (T_S) and (θ_D) temperatures increased with only a slight decrease observed at $y = 2$

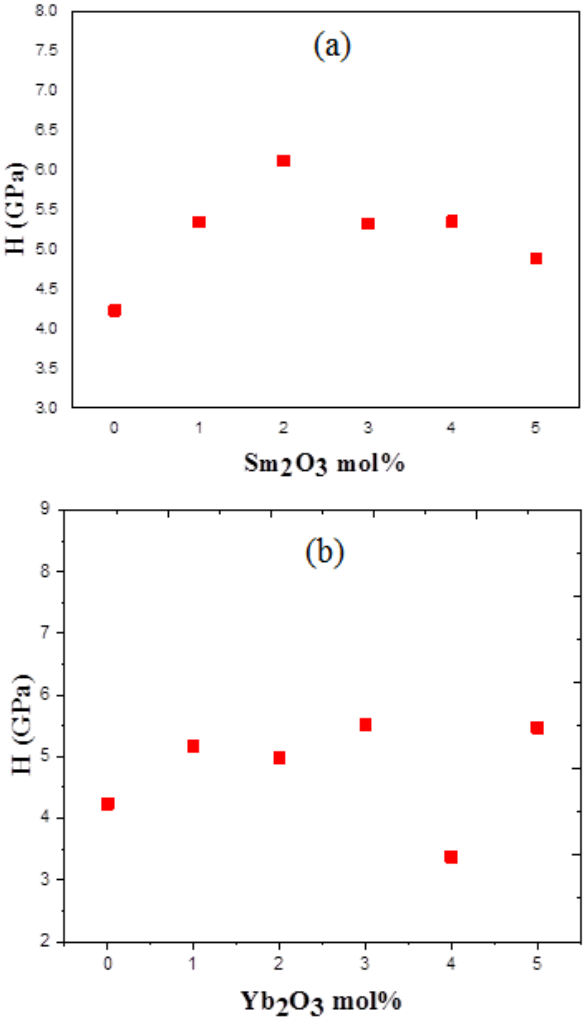

Figure 7. Micro hardness (H) of (a) TWSm glasses and (b) of TWYb glasses.

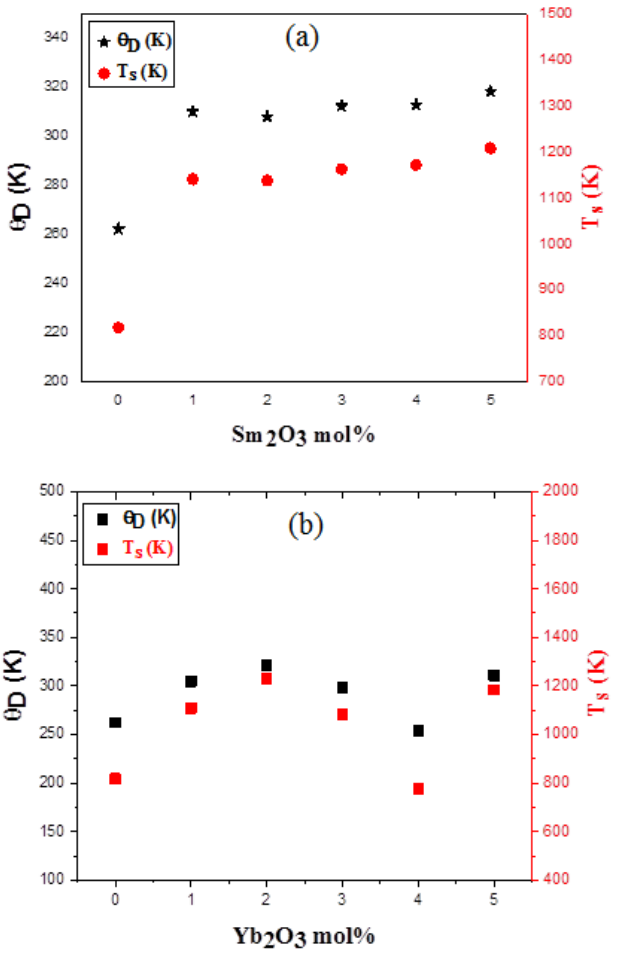

Figure 8. Debye and softening temperatures of (a) TWSm glass system and (b) Debye and of TWYb glass system.

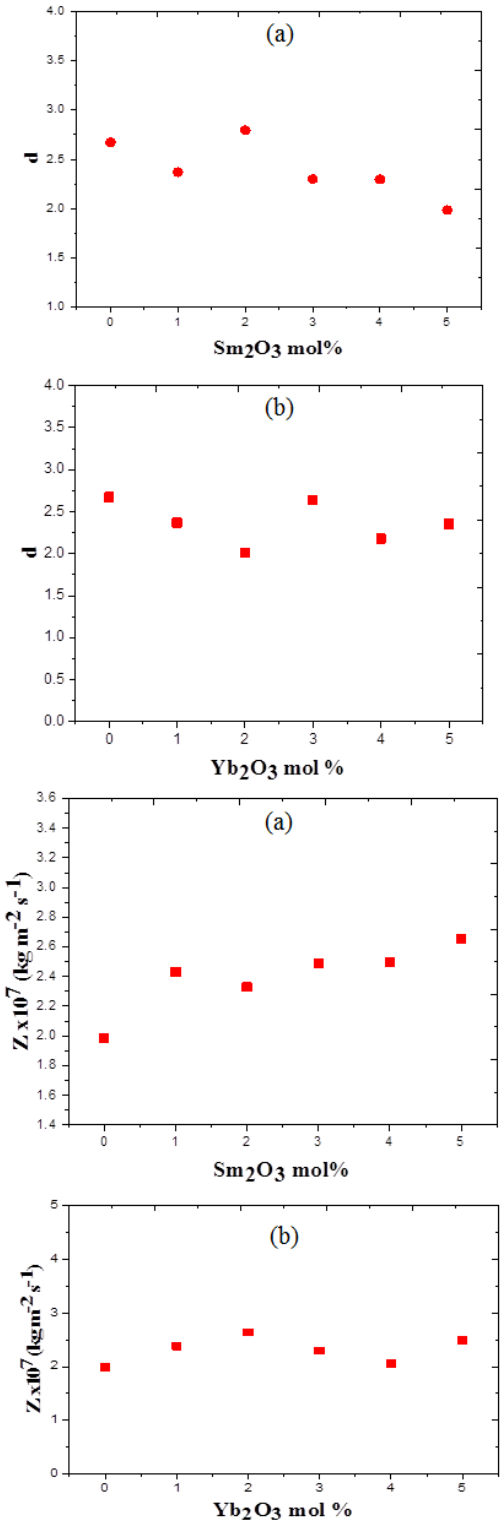

Figure 9. (a) Fractal bond connectivity d, acoustic impedance Z for TWSm glasses and (b) for TWYb glasses.

mole% with an increase in Sm^{3+} content and their values varied from $262-318$ (K) and $817-1207$ (K) respectively. But for TWYb system, their values are found in the range $262-310$ (K) and $817-1183$ (K) respectively. The reduction of (θ_D) and (T_S) temperatures depend on the number of atoms/unit volume and the presence of NBOs in the glass system [20–36].

The behavior of (d) and (Z) of the two glass series (TWSm) and (TWYb). It can be observed that for (TWSm) samples, parameter (d) decreased from 2.67 to 2.37 and 2.30 to 1.98 respectively with an increase in Sm^{3+} content. Meanwhile, the acoustic impedance (Z) increased from 1.99×10^7 to 2.65×10^7 (Kg m^{-2} s^{-1}) with an increase in Sm^{3+} content. For the other system (TWYb), parameter (d) exhibits a decreasing trend with only a slight increase observed with an increase in Yb^{3+} content. The acoustic impedance (Z) showed an increasing trend from 1.99×10^7 to 2.64×10^7 (Kg m^{-2} s^{-1}) with an increase in Yb^{3+} content and then decreased to 2.01×10^7 (Kg m^{-2} s^{-1}) at concentration 4 mol%. The decreasing values for fractal bond connectivity (d) can be linked to the increase in the amount of BOs and the decline in glass rigidity, respectively. Fractal bond connectivity (d) values only increase when $y = 2.0$ M fractions. The increase in (d) indicates an increase in the number of NBOs [20–36]. Because of the high demand for communications, rise the development of potential glass materials for optical communications and the current data is crucial. The present outcome will complete the previous work on TeO_2-WO_3 glass system with different modifiers such as

GeO_2, Ag_2O and Bi_2O_3 [37–39].

4. Conclusion

Because, mechanical properties are crucial parameter in manufacturing optical fibers, two glass series (TWSm) and (TWYb) were successfully synthesized. The outcome of this work can be summarized through the following points:
1. Both (ρ) and (V_M) increased with the increasing of dopants (Sm^{3+}) or (Yb^{3+}) concentration in both glass series,
2. Longitudinal V_L, and shear V_S velocities were examined and found in the range from 3309 to 4337 (ms^{-1}), 3309 to 4061 (m^{-1}), and 1967 to 2370 (m^{-1}), 1967 to 2332 (m^{-1}) for TWSm and TWYb , respectively,
3. The (L), (G), (K), and (E) show a similar trend with ultrasonic velocities with the increment of the Sm^{3+} or Yb^{3+} concentrations. Moreover, the bulk modulus of (TWSm) is higher than that of (TWYb) glass,
4. The (σ) range from 0.227 to 0.287 for TWSm and from 0.227 to 0.287 for TWYb glasses,
5. The (H) range 4.23 GPa to 6.12 GPa for Sm samples and from 4.23 GPa to 5.51 GPa for Yb samples with the addition of dopants, which indicates the rigidity of the glass sample has been improved,
6. Both (θ_D) and (T_S) temperatures were found in the range from 262 to 318 and 817 to 1207 K for (TWSm) and from 262 to 310 and 817 to 1183 K for (TWYb), respectively. The rising values of (θ_D) and (T_S) temperatures can be predicted as a result of the strengthening of the glass structure which is due to the generation of BO,
7. The (d) showed a decreasing behavior with the addition of the Sm^{3+}.

Conflict of interest statement:
The authors declare that they have no conflict of interest.

References

[1] A. Lira, G. V. Vázquez, I. Camarillo, U. Caldi no, G. Mu noz H, J. Orozco, J. L. Ruvalcaba, and M. Manrique Ortega. "High laser performance of an Al^{3+} and Nd^{3+}-codoping in a sodium-borotellurite glass for NIR broadband laser application". *Journal of Luminescence*, **255**:119545, 2023.

[2] D. Vijayasri, K. S. Rudramamba, T. Srikanth, N. Mahendra Reddy, Mamatha Nakka, S. Pratyusha, and M. Rami Reddy. "Spectroscopic features of Tb^{3+} doped strontium zinc borate glasses for green laser applications". *Journal of Molecular Structure*, **1274**:134514, 2023.

[3] J. Wang, Z. Jia, C. Zhang, Y. Sun, Y. Ohishi, W. Qin, and G. Qin. "Thulium-doped fluorotellurite glass fibers for broadband S-band amplifiers". *Optics Letters*, **47**:1964, 2022.

[4] A. Aşkın, M. I. Sayyed, Amandeep Sharma, M. Dal, R. El-Mallawany, and M. R. Kaçal. "Investigation of the gamma ray shielding parameters of (100-x)[0.5 Li_2O–0.1 B_2O_3–0.4 P_2O_5]-xTeO_2 glasses using Geant4 and FLUKA codes". *Journal of Non-Crystalline Solids*, **521**:119489, 2019.

[5] A. Andrianov and E. A. Anashkina. "Thermo-optical control of L-band lasing in Er-doped tellurite glass microsphere with blue laser diode". *Optics Letters*, **47**:2182, 2022.

[6] R. El-Mallawany. "Longitudinal elastic constants of tellurite glasses". *Journal of Applied Physics*, **73**:4878, 1993.

[7] R. N. Hampton, W. Hong, G. A. Saunders, and R. A. El-Mallawany. "Dielectric properties of tellurite glass". *Physics and Chemistry of Glasses*, **29**:100, 1988.

[8] M. P. Belançon, M. Sandrini, H. S. Muniz, L. S. Herculano, G. V. B. Lukasievicz, E. L. Savi, O. A. Capeloto, L. C. Malacarne, N. G. C. Astrath, M. L. Baesso, G. J. Schiavon, A. A. Silva Junior, and J. D. Marconi. "Float, borosilicate and tellurites as cover glasses in Si photovoltaics: Optical properties and performances under sunlight ". *Journal of Physics and Chemistry of Solids*, **161**:110396, 2022.

[9] L. Niu, H. Shi, Y. Ye, C. Liu, B. Jia, Y. Chu, L. Liu, J. Ren, and J. Zhang. "Optimized tellurite glasses containing $CsPbBr_3$-quantum dots for white-light emitting diodes". *Journal of Non-Crystalline Solids*, **581**:121429, 2022.

[10] M. A. Sidkey, R. A. El Mallawany, A. A. Abousehly, and Y. B. Saddeek. "Relaxation of longitudinal ultrasonic waves in some tellurite glasses". *Materials Chemistry and Physics*, **74**:222, 2002.

[11] N. Elkhoshkhany, R. El-Mallawany, and E. Syala. "Mechanical and thermal properties of TeO_2–Bi_2O_3–V_2O_5–Na_2O–TiO_2 glass system". *Ceramics International*, **42**:19218, 2016.

[12] R. N. Hampton, W. Hong, G. A. Saunders, and R. A. El-Mallawany. "The electrical conductivity of pure and binary TeO_2 glasses". *Journal of Non-Crystalline Solids*, **94**:307, 1987.

[13] R. El-Mallawany, A. Abousehly, A. A. El-Rahamani, and E. Yousef. "Radiation effect on the ultrasonic attenuation and internal friction of tellurite glasses". *Materials Chemistry and Physics*, **52**:161, 1998.

[14] H. Mh Zakaly, A. S. Abouhaswa, S. A M Issa, M. Y. A Mostaf, M. Pyshkina, and R. El-Mallawany. "Optical and nuclear radiation shielding properties of zinc borate glasses doped with lanthanum oxide". *Journal of Non-Crystalline Solids*, **543**:120151, 2020.

[15] P. Sailaja, Sk. Mahamuda, K. Swapna, M. Venkateswarlu, and A. S. Rao. "Near-infrared photoluminescence studies of neodymium ions doped SrO-Al_2O_3-$BaCl_2$-B_2O_3-TeO_2 glasses for laser and fiber amplifier applications". *Optics and Laser Technology*, **156**:108569, 2022.

[16] Y. Morova, M. Khan, B. Denker, B. Galagan, S. Sverchkov, and A. Sennaroglu. "Tunable continuous-wave laser operation of Tm^{3+} ion doped tellurite glass near 2 μm". *Journal of Luminescence*, **252**:119318, 2022.

[17] P. Wang, Y. Cui, S. Zhao, R. Ye, M. Cai, L. Calvez, J. Rocherulle, F. Huang, H. Ma, G. Bai, J. Zhang, S. Xu, and X. Zhang. "Effects of melting temperature on color-changing in germano-tellurite niobate glass". *Optics and Laser Technology*, **156**:108627, 2022.

[18] D. Tang, Y. Tian, D. Dorosz, X. Wang, X. Yang, Y. Liu, X. Zhang, J. Zhang, and S. Xu. "2–3 μm mid-infrared luminescence of Ho^{3+}/Yb^{3+} co-doped chloride-modified fluorotellurite glass". *Spectrochimica Acta Part A: Molecular and Biomolecular Spectroscopy*, **285**:121833, 2023.

[19] M. Dolhen, M. Tanaka, V. Couderc, S. Chenu, G. Delaizir, T. Hayakawa, J. Cornette, F. Brisset, M. Colas, P. Thomas, and J. Duclère. "Nd^{3+}-doped transparent tellurite ceramics bulk lasers". *Scientific Reports*, **8**:4640, 2018.

[20] R. A. El-Mallawany and G. A. Saunders. "Elastic behavior under pressure of the binary tellurite glasses TeO_2-$ZnCl_2$ and TeO_2-WO_3". *Journal of Materials Science Letters*, **6**:443, 1987.

[21] R. A. El-Mallawany and G. A. Saunders. "Elastic properties of binary, ternary and quaternary rare earth tellurite glasses". *Journal of Materials Science Letters*, **7**:870, 1988.

[22] R. El-Mallawany, M. Sidkey, A. Khafagy, and H. Afifi. "Elastic constants of semiconducting tellurite glasses". *Materials Chemistry and Physics*, **37**:295, 1994.

[23] R. El-Mallawany and A. Abd El-Moneim. "Comparison between the elastic moduli of tellurite and phosphate glasses". *Physica Status Solidi (a)*, **166**:829, 1998.

[24] R. El-Mallawany. "Quantitative analysis of elastic moduli of tellurite glasses". *Journal of Materials Research*, **5**:2218, 1990.

[25] R. El-Mallawany, A. El Adawy, A. Gamal, and Y. S. Rammah. "Experimental and theoretical elastic moduli of sodium–zinc–tellurite glasses". *Optik*, **243**:167330, 2021.

[26] R. El-Mallawany, M. S. Gaafar, and N. Veeraiah. "Evaluation of bulk modulus and ring diameter of some tellurite glass systems". *Chalcogenide Letters*, **12**:67, 2015.

[27] Y. A. Abdelghany, M. M. Kassab, M. M. Radwan, and A. Abdel-Latif M. "Investigation of optical, mechanical, and shielding properties of zirconia glass capsule". *Progress in Nuclear Energy*, **154**:104457, 2022.

[28] J. S. Alzahrani, S. N. Nazrin, C. Eke, I. Kebaili, M. S. Al-Buriahi, and A. S. J. Syaiwan. "Effect of strontium oxide on radiation shielding features and elastic properties on zinc borotellurite glass system". *Radiation Physics and Chemistry*, **199**:110304, 2022.

[29] N. Tamam, Z. A. Alrowaili, A. Hammoud, A. V. Lebedev, I. Boukhris, I. O. Olarinoye, and M. S. Al-Buriahi. "Mechanical, optical, and gamma-attenuation properties of a newly developed tellurite glass system". *Optik*, **266**:169355, 2022.

[30] M. I. Sayyed, N. S. Prabhu, J. F. M. Jecong, and S. D. Kamath. "Radiation shielding analysis using EPICS2017 and mechanical property characterization of zinc boro-tellurite alumina glasses". *Optik*, **257**:168814, 2022.

[31] M.I. Sayyed, M. Kh Hamad, M.H.A. Mhareb, N. S. Prabhu, H. Khosravi, and S. D. Kamath. "Effect of different modifiers on mechanical and radiation shielding properties of SrO-B_2O_3-TeO_2 glass system". *Optik*, **257**:168823, 2022.

[32] C. Devaraja, G. V. J. Gowda, B. Eraiah, and G. K. N. Murthy. "Elastic properties of boro-tellurite glasses doped with europium oxide". *Journal of Metals, Materials and Minerals*, **32**:56, 2022.

[33] N. Alfryyan, Z. A. Alrowaili, H. H. Somaily, I. O. Olarinoye, N. Alwadai, C. Mutuwong, and M. S. Al-Buriahi. "Comparison of radiation shielding and elastic properties of germinate tellurite glasses with the addition of Ga_2O_3". *Journal of Taibah University for Science*, **16**:183, 2022.

[34] N. N. S. Nidzam, H. M. Kamari, M. S. M. Sukari, F. A. M. Alauddin, H. Laoding, M. N. Azlan, S. Wei Hann, N. M. Al-Hada, and I. Boukhris. "Comparison study of elastic, physical and structural properties for strontium oxide and manganese oxide in borotellurite glasses for high strength glass application". *Journal of Inorganic and Organometallic Polymers and Materials*, **32**:353, 2022.

[35] A. Moneium and R. El-Mallawany. "Nb_2O_5–TeO_2 and Nb_2O_5–Li_2O–TeO_2 glasses: Evaluation of elastic properties". *Journal of Non-Crystalline Solids*, **575**:121229, 2022.

[36] A. D'Souza, B. Padasale, M. S. Murari, N. Karunakara, M. I. Sayyed, M. Elsafi, H. Al-Ghamdi, A. H. Almuqrin, and S. D. Kamath. "TeO_2 for enhancing structural, mechanical, optical, gamma and neutron radiation shielding performance of bismuth borosilicate glasses". *Materials Chemistry and Physics*, **293**:126657, 2023.

[37] N. Ghribi, M. Dutreilh-Colas, J.-R. Duclère, F. Gouraud, T. Chotard, R. Karray, A. Kabadou, and P. Thomas. "Structural, mechanical and optical investigations in the TeO_2-rich part of the TeO_2-GeO_2-ZnO ternary glass system". *Solid State Sciences*, **40**:20, 2015.

[38] M. M. Umair, A. K. Yahya, M. K. Halimah, and H. A. A. Sidek. "Effects of increasing tungsten on structural, elastic and optical properties of xWO_3-(40-x)Ag_2O-60Te_2O glass system". *Journal of Materials Science and Technology*, **31**:83, 2015.

[39] H. A. Thabit, A. K. Ismail, H. Es-soufi, D. A. Abdulmalik, A. M. Al-Fakih, S. Alraddadi, and M. I. Sayyed. "Structural, thermal, and mechanical investigation of telluro-borate-Bismuth glass for radiation shielding". *Journal of Materials Research and Technology*, **24**:4353, 2023.